

# Application of Norland adhesive for holographic recording

L. Goldenberg<sup>a,b,\*</sup>, O. Sakhno<sup>a</sup>, J. Stumpe<sup>a,b</sup>

<sup>a</sup> *Fraunhofer Institute for Applied Polymer Research, Science Campus Golm, Geiselbergstr. 69, 14476 Potsdam, Germany*

<sup>b</sup> *Institute of Thin Film Technology and Microsensorics, 14513 Teltow, Germany*

Received 28 May 2004; accepted 24 September 2004

Available online 6 November 2004

## Abstract

Norland UV-adhesive NOA68 was studied as a material for holographic optical elements fabrication. Permanent transmission diffractive gratings were inscribed by the exposure to the interference field of UV Ar-ion laser. The contributions of the volume and the surface parts of the phase modulation to the efficiency of the gratings were investigated for different gratings periods. The depth of the surface relief grows up to 250 nm with an increase in the grating period. For relatively small periods  $\leq 2.5 \mu\text{m}$  the contribution of the surface relief part to the total diffraction efficiency is negligible and gratings can be considered as volume diffractive structures. The deep (up to  $1.5 \mu\text{m}$ ) surface relief with almost square profile was manufactured by the UV exposure through a mask. Both techniques do not require any subsequent wet or thermal developing process. The mechanism of the holographic image formation is discussed.

© 2004 Elsevier B.V. All rights reserved.

PACS: 42.70.Ln

Keywords: Holographic recording materials; Photopolymerisation; Diffraction gratings

## 1. Introduction

Holographic and diffractive optical technology is of great interest for integrated optics, optical data storage, optical interconnects, optical computers, etc. Photopolymers are promising materials for the holographic and lithographic fabrication of the optical elements. Until now, numerous photopolymeric materials including DuPont acrylate solid photopolymer films [1,2], acrylamide based compositions [3], phenanthrenequinone-dye doped poly(methyl methacrylate) [4], multicomponent acrylate oligomer-monomer and oligomer-diluents liquid mixtures [5–9], and polymers containing azobenzene moieties [10,11] were used as the holographic recording media. In the most of these

materials only volume phase periodic structure forms, two last ones may insure the formation of both volume and surface relief patterns. Photopolymerisation, diffusion of one or more components, photoinduced addition or photoisomerisation are plausible mechanisms of the image formation in the photopolymers.

Optical adhesives, produced, for example, by Norland Corporation (NOA), are quickly polymerised upon UV irradiation and usually used for gluing of the optical components to each other or to metal. However, such adhesives themselves can be used for the manufacture of the optical diffractive elements.

The most attractive feature of the NOA adhesives as materials for optical element fabrication is the absence of any chemical or thermal processing before and after imaging procedure. One of these commercial materials (NOA65) was recently used for the fabrication of the computer generated gratings and kinoforms [12]. The fabrication of these diffractive optical elements was performed by lithographic technique. Some examples of

\* Corresponding author. Address: Fraunhofer Institute for Applied Polymer Research, Science Campus Golm, Geiselbergstr. 69, 14476 Potsdam, Germany.

E-mail address: [goldenberg@iap.fhg.de](mailto:goldenberg@iap.fhg.de) (L. Goldenberg).

kinoform patterns with relatively good efficiency have been reported [12]. In addition the material was recently used to fabricate holographic polymer dispersed liquid crystals (H-PDLC) structures. The mechanism of polymerisation, phase separation of LC and the formation of the holographic gratings due to the periodic distribution of LC-droplets within polymer films during the exposure were discussed in details [13].

The Norland adhesives are generally mixtures of multifunctional aliphatic thiols, vinyl monomers and photoinitiator [12,13]. The irradiation with UV light (200–400 nm) results in polymer network formation due to thiol-radicals addition to the double bond of vinyl component. From the chemistry itself and from the published results [12] it is not clear so far whether the exposure to the interference light field or through a mask would lead to the volume and/or the surface relief structure formation in the film. The second open question is whether a surface relief structure may be obtained without subsequent development of the film or with an additional post-processing.

In this article we report one-step procedure to fabricate the phase diffractive gratings using NOA68. Holography and lithography were applied as rather simple techniques. The influence of the parameters of these procedures on the final gratings is reported. Diffractive properties of the fabricated structures were tested and analysed. The mechanism of the image formation is also discussed.

## 2. Experimental

In most experiments NOA68 adhesive (Norland Corporation) as the recording material was used. The films were prepared by spin-coating of the weighted amount of NOA68 onto the glass substrates of known size at 2000–3000 rpm. The films thickness was measured after holographic exposure using DEKTAK profilometer (Veeco, USA).

Ar-ion laser (Spectrophysics, model BeamLok 2080) with  $\lambda_{\text{rec}} = 364 \text{ nm}$  and output power of  $\sim 500 \text{ mW}$  was used for the holographic exposure. An experimental set-up consists of a shutter, a spatial filter, collimating lens, a 50:50 beam-splitter and two plane mirrors. Transmission gratings with fringes perpendicular to a polymer plane were recorded by the exposure of the films to the interference pattern of two coherent planar waves (*s*-polarization) intersecting in the sample plane. The intensity balance between two recording beams was near 1:1. The spatial frequency of the gratings recorded (grating period,  $\Lambda$ ) was changed by varying the angle between the recording beams. A He-Ne laser ( $\lambda_{\text{test}} = 633 \text{ nm}$ , *s*-polarisation) was used as a probe beam to test the grating formation. The power of the first-order diffracted,  $P_{\text{dif}}(t)$ , and transmitted,  $P_{\text{trans}}(t)$ , beams

were measured using two photodiodes. The kinetics of the recording process was monitored by the time behaviour of the gratings diffraction efficiency ( $\text{DE}(t)$ ), determined as  $\eta(t) = P_{\text{dif}}(t)/(P_{\text{dif}}(t) + P_{\text{trans}}(t))$ . Such determination of DE characterises the holographic properties of material only (amplitude of the phase modulation) and does not take into consideration the losses associated with Fresnel reflection and a light-scattering of a substrate. In all experiments the holographic exposure was terminated upon achieving the saturation of the diffraction efficiency. The recording and testing processes were controlled by PC software developed in-house. The program controls the shutter, data acquisition from the photodiodes, and simultaneous calculation of DE in real time.

The striped patterned photomasks with the periods of 15 and  $6 \mu\text{m}$  were used for the lithographic exposure.

The surface of the exposed NOA films was examined by Atomic Force Microscopy with Solver P47H Smena (NTMDT, Russia).

## 3. Results and discussion

The absorption spectrum of the NOA68 layer is shown in the Fig. 1. Ar-ion laser light emitted at wavelength 364 nm could be used to initiate the photochemical reactions and physical processes leading to the gratings formation in NOA68. After irradiation the material exhibits high rigidity and high transparency in the whole VIS region of the spectrum, allowing the fabrication of the optical elements.

The relatively low viscosity of the starting material and its poor wetting of the glass substrate did not allow to form a flat surface after spin-coating, which results in some thickness variation. Typically the thickness varied in the range of 30–33  $\mu\text{m}$  for the different samples. Besides a shallow noise structure was usually observed on the surface of gratings and a weak noise pattern

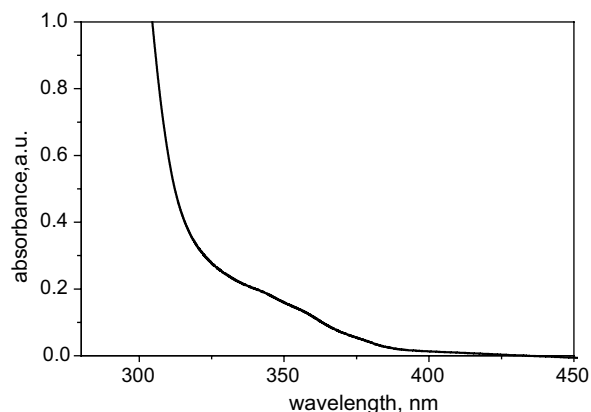


Fig. 1. Absorbance of unexposed NOA68 layer ( $d \approx 30 \mu\text{m}$ ).

was presented in the diffraction picture. Probably, it is associated with some chemical reactions accompanied by the gas product evolution.

The influence of the recording intensity on the final value of the DE was studied for the gratings of different periods. For example, typical kinetics of the gratings (period  $\Lambda = 0.85 \mu\text{m}$ ) inscription submitted to the different exposure conditions (intensity of the recording beams) are shown in the Fig. 2. It was found, that final DE increases under increase in the recording intensity, with the maximum being observed for the intensity near  $50 \text{ mW/cm}^2$ . Further increasing in the recording intensity (from 50 to  $70 \text{ mW/cm}^2$ ) did not change the value of the final DE. The higher intensity of the writing beam the faster saturation value of the DE may be achieved. The maximum DE could be obtained only with high writing intensity (Fig. 2). Such a trend was valid for the periods in the range of  $0.3\text{--}3 \mu\text{m}$ .

The obtained features of the recording process are discussed below in detail, in association with the proposed mechanism of the grating formation. The recording process carried out under higher intensities posses the advantages of maintaining higher rate of the photopolymerisation in the bright regions of the interference field, and probably, higher difference of the refractive index in the neighbouring areas of the grating.

As reported in [12] the non-homogeneous light exposure of NOA65 layers led to the formation of the volume and surface relief structures. We have found the same situation for NOA68. Testing the surface of the gratings by means of AFM has shown the presence of the surface relief structure for all periods studied. However, the features of the diffractive pattern (the presence of only two diffraction orders and high diffraction efficiency for the smaller periods) evident the periodic modulation of the material refractive index. It was revealed that the holographic recording in the NOA68 layers is accompanied by the formation of both volume and surface relief structures.

Both surface relief and volume (refractive index) modulation of the material provide their own contribu-

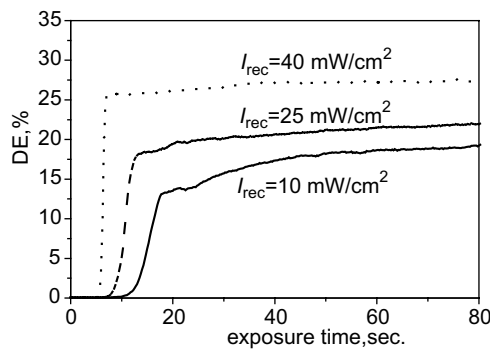


Fig. 2. Kinetics of the gratings recording in the NOA68 film for different intensities of the recording beams ( $\Lambda = 0.85 \mu\text{m}$ ).

tions to the diffraction efficiency of the gratings at almost all periods tested. The total phase shift of the light passing through such volume-surface gratings can be determined as:

$$\Delta\delta_{\text{total}} = \Delta\delta_{\text{vol}} + \Delta\delta_{\text{surf}} \quad (1)$$

where  $\Delta\delta_{\text{vol}}$ ,  $\Delta\delta_{\text{surf}}$  are the relative phase differences of light passing through two adjacent regions of the volume and the surface relief gratings consequently.

Investigation of both components of the phase modulation versus recording intensity, grating period and post-processing treatment were performed and discussed below.

Experimental results show that for each period studied both total DE and depth of the surface relief ( $h$ ) typically achieve a certain saturation value under increase in the recording intensity. Such dependency for the gratings with  $\Lambda = 0.85 \mu\text{m}$  is shown in the Fig. 3. The total DE does not exceed 40% and the obtained value of  $h$  was not higher than 28 nm.

Different types of the diffractive gratings are formed under the irradiation with the periodic light field of the different spatial frequency. Two types of diffraction is customarily distinguished by defining a dimensionless Cook–Klein parameter  $Q$  [14]):

$$Q = 2\pi\lambda_{\text{test}}d/n\Lambda^2, \quad (2)$$

where  $d$  is the thickness of the grating,  $\Lambda$  is the grating period,  $n$  is the spatially averaged refractive index of the recording medium, and  $\lambda_{\text{test}}$  is the incident wavelength. A “thick” or volume gratings ( $Q \geq 10$ ) correspond to the Bragg diffraction and provide the diffraction when incident angle satisfies the phase matching conditions [14]. Such structures exhibit only two diffraction orders (zero- and the first-order) and a strong dependency of the DE on the angle and wavelength of the incident light. The DE of the transmission volume phase grating in Bragg conditions is described by:

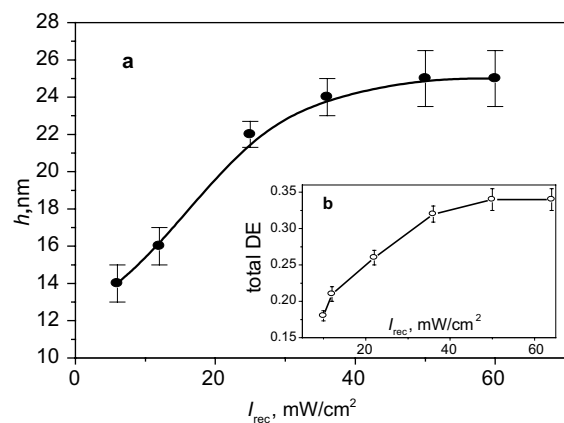


Fig. 3. Total DE and surface relief depth  $h$  versus recording intensity ( $\Lambda = 0.85 \mu\text{m}$ ).

$$\eta_{\text{vol}} = \sin^2(\Delta\delta_{\text{vol}}/2) = \sin^2(\pi n_1 d / \lambda_{\text{test}} \cos \theta_0) \quad (3)$$

where  $n_1$  is the amplitude of refractive index modulation of the material,  $\theta_0$  is the Bragg angle of the incident light within the material.

On the other hand, “thin” gratings ( $Q \leq 1$ ) correspond to the Raman–Nath regime of the optical diffraction. In this regime, many orders of diffraction can be observed. The efficiency of the first-order Raman–Nath diffraction for the grating with a sinusoidal modulation of refractive index is given by

$$\eta_{\text{surf}} = J_1^2(\Delta\delta_{\text{surf}}/2) = J_1^2(2\pi h(n_{\text{I}} - n_{\text{II}})/\lambda_{\text{test}}) \quad (4)$$

where  $J_1^2(\Delta\delta_{\text{surf}}/2)$  is the first-order Bessel functions of the first kind,  $h$  is the depth of the grating grooves, and  $n_{\text{I}}$ ,  $n_{\text{II}}$  are the refractive indices of the adjacent areas of the grating [14].

The gratings of the periods 0.3–1.5  $\mu\text{m}$  exhibit typical properties of the Bragg gratings: only two diffraction orders were observed and the DE of the gratings was dependent strongly on the incident angle of the probe beam. These gratings were “thick” according to the value of Cook–Klein parameter, which varied from 860 to 30 for the periods 0.3 and 2  $\mu\text{m}$ , respectively. The diffraction pattern of the gratings with the periods 4–8  $\mu\text{m}$  exhibit more than two diffraction orders and weak dependence of the DE on the angle of the incident beam.

The efficiency of the first-order diffraction for the gratings with period 0.3–2.5  $\mu\text{m}$ , recorded with almost equal recording intensities, is shown in the Fig. 4. The maximum DE was observed for the gratings with periods 0.7–1.5  $\mu\text{m}$ ; DE drops for the period below 0.5  $\mu\text{m}$  and above 2  $\mu\text{m}$  (where the gratings transform from the “thick” into the intermediate or “thin” type).

The dependence of the relief depth  $h$  on the period is presented in the Fig. 5. Generally, for larger periods deeper surface relief could be inscribed in the film. Maximum depth of surface relief achieved was  $\approx 250$  nm at  $\Lambda = 7.5$   $\mu\text{m}$ .

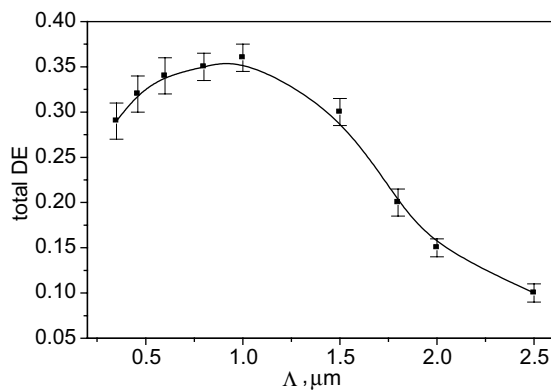


Fig. 4. Total DE versus period (recorded with the comparable intensities ( $d \approx 32$   $\mu\text{m}$ )).

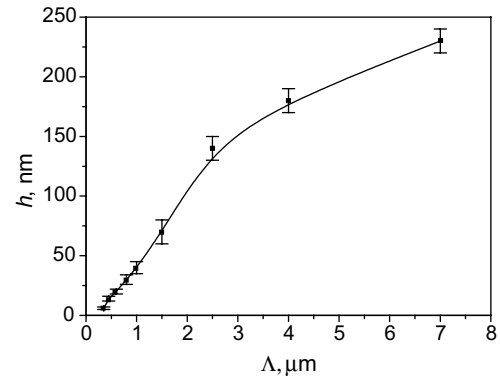


Fig. 5. Maximum  $h$  versus grating period (recorded with the comparable intensities).

The measured dependency of the amplitude of the refractive index modulation  $n_1$  versus period is presented in the Fig. 6. The measurements were carried out using the immersion liquid ( $n_{\text{im}} \approx n_{\text{pol}}$ , for NOA68  $n_{\text{pol}} = 1.54$ ) on the surface of the gratings in order to eliminate the surface relief modulation contribution into the total efficiency. In such conditions the total efficiency, especially for the periods 0.3–1.5  $\mu\text{m}$ , exhibits a negligible decline compare to the measurements without the immersion liquid. This evidences the dominant role of the refractive index modulation in the formation of the holographic gratings for the mentioned periods. The values of  $n_1$  were calculated from the measured values of DE using the Eq. (3). The refractive index modulation decreases slightly for the smaller periods, achieves maximum value for  $\Lambda = 0.7$ –1  $\mu\text{m}$ , and then drops slowly with the increase in the gratings period. This behaviour is correlated with the dependence of the total DE on the period (Fig. 4).

AFM images of the gratings with the different periods (Fig. 7) evident that the surface relief has almost sinusoidal profile. Thus the efficiency of these relief gratings can be estimated approximately using Eq. (4), where  $n_{\text{I}} = n_{\text{pol}}$ ,  $n_{\text{II}} = n_{\text{air}}$ . Our calculations revealed that for  $\Lambda = 0.3$ –2.5  $\mu\text{m}$  the contribution of the relief into the

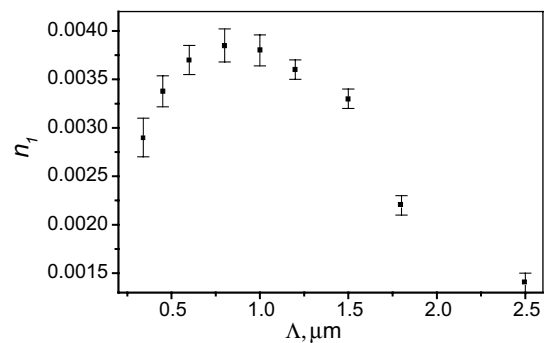


Fig. 6. Dependence of the amplitude of refractive index modulation ( $n_1$ ) versus grating period.

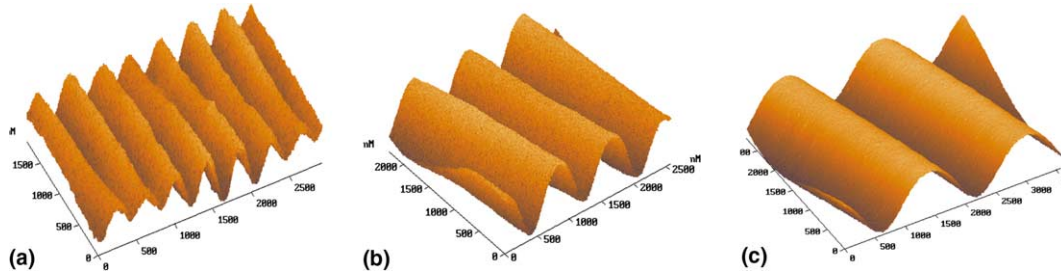


Fig. 7. AFM images (semi-contact mode) of the surface relief gratings with different periods: (a) 4000 nm; (b) 750 nm; (c) 1510 nm.

total DE is negligibly small, that correlates to the measured values of  $n_1$  presented above. Even for the gratings with  $\Lambda = 1.5 \mu\text{m}$  and  $h \approx 50 \text{ nm}$  the efficiency due to the surface relief modulation does not exceed 2%. Only for larger periods ( $\Lambda \geq 5 \mu\text{m}$ ) with  $h = 200 \text{ nm}$  and higher, the refractive index modulation becomes negligible and the diffraction efficiency is determined by the surface relief modulation mainly.

Thus, NOA68 insures in situ holographic fabrication of the volume phase gratings in the period range of 0.3–3  $\mu\text{m}$ , where the influence of the surface relief modulation is negligible. The exposure of NOA68 layers to the interference field of the periods higher than 3  $\mu\text{m}$  causes the sinusoidal surface relief formation with sufficiently deep grooves, those parameters determine the grating efficiency.

It was found that the surface relief formation in NOA68 occurs during the holographic exposure and does not require any post-development. Moreover, our attempts to develop the exposed NOA gratings with different solvents (alcohol, acetone), which dissolve the original adhesive, resulted in the peel off the film from the substrate. A post-exposure annealing of the NOA-gratings up to 60 °C does not change the total DE and depth of the surface relief. Heating up to 110 °C reduces the height of the relief from 10 to 1.5 nm (for the gratings with  $\Lambda = 0.4 \mu\text{m}$ ) and almost does not change the total DE.

It was observed that the increase in thickness of the recording layers up to 60  $\mu\text{m}$  ( $\Lambda = 1 \mu\text{m}$ ) is accompanied by the increase in the DE of a volume grating up to 70%. However, the depth of the surface relief did not show any further increase under these conditions.

Pure volume refractive index gratings can be recorded in the layers of NOA68 placed between two glass substrates, when substrates prevent the relief formation. The thickness of the film is controlled by the special spacers. The experiments revealed that the DE of such gratings is typically lower than the DE of the gratings of the same period, fabricated with a free surface. For example, the grating with  $\Lambda = 1 \mu\text{m}$  exhibits DE  $\approx 45\%$  in the film with a free surface and DE  $\approx 20\%$  in the film between two substrates (the same thickness of the films). Thus the holographic recording between two substrates

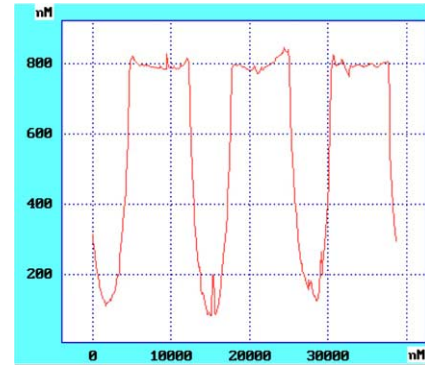


Fig. 8. Cross-section of the AFM image (contact mode) of the structure obtained by the photolithography with the amplitude mask of 15  $\mu\text{m}$  period.

causes smaller phase modulation compare to the films with a free surface. The reason of such effect is discussed below.

The exposure of the adhesive layers to the square light distribution through the amplitude masks (photolithography) with period from 1 to 15  $\mu\text{m}$  led to the relief structure formation with the depth up to 1.5  $\mu\text{m}$  (in the case of 15  $\mu\text{m}$  period) and almost square profile (Fig. 8).

It could be concluded from the AFM images of the holographic and lithographic gratings of the different periods that NOA adhesives have relatively linear response to the light distribution in the irradiation field (sinusoidal profile for the holographic exposure and square profile for the lithographic irradiation). This may be useful in respect to the application of NOA68 as a material for the fabrication of surface relief structures. In contrast to the well-known photoresists the diffractive structures in NOA68 do not require any pre- and post-processing treatment of the relief.

#### 4. Mechanism of the image formation in NOA68

The mechanism of the holographic recording in the NOA68 layers is not well understood so far. However, the experimental results (dependencies of the DE, amplitude of refractive index modulation  $n_1$  and depth of the

relief  $h$  on the different recording parameters) allow to discuss possible processes involved in the volume and relief modulation.

Several holographic multi-component initially liquid or low-viscose photopolymer materials, their parameters and mechanism of the holographic image formation were presented so far in the literature [3,6–8]. Two main processes of the image formation may be involved simultaneously. The first one is the photopolymerisation reaction itself. Different degree of the monomer conversion and different cross-linking density in the bright and dark zones of the interference field results in the modulation of the material density, and, consequently, the refractive index. Thus, this process leads to the volume refractive index grating formation. From the other hand the gradient in the material density results in the periodic change of the material shrinkage (the formation of surface relief structure).

The second process is a photo-induced mass-transport of the component(s) during holographic exposure, that is typical, for example, for the multi-component acrylate or acrylamide formulations [3,6–8]. In this case the components that possess higher reactivity and/or higher rate of diffusion move from the dark to bright areas (or vice versa) creating a concentration gradient. This also causes the refractive index modulation and/or relief formation as well.

The contribution of each of these processes should be dependable on the writing intensity and the period of the structure.

The experimental results, for example, growth of the efficiency of the volume gratings on the recording intensity, confirm the contribution of the first process. The intensity difference in the bright and dark zones increases with the increase in the writing intensity. This results in a higher difference of polymer cross-linking density [15,16], and, according to the first process, higher DE, respectively (Fig. 4).

The dependence of  $n_1$  on the period may be also helpful for the mechanism elucidation (Fig. 6). The curve

exhibits a peak value of  $n_1$  for  $\Lambda = 0.4–1.2\ \mu\text{m}$  (gratings were recorded with the comparable recording intensity), a weak decay in the range of smaller period, and a strong drop for the large periods. Almost constant and high  $n_1$  is well explained by the first process. The weak decrease of  $n_1$  for smaller periods could be due to polymer chain growth into adjoining dark areas, resulting in so called “smearing” of the refractive index profile. This type of the material response was described as a non-local [3], since refractive index change initiated at one position, produces a change at a point some distance away. The decrease of  $n_1$  for the larger periods can be explained by the contribution of the second, mass-transport process to the image formation. The following considerations probably may be helpful at this point.

The gel-point in the thiolene formulations is reached typically after 50% monomer conversion (in comparison to the acrylate systems with the gel-point at 5% of the general conversion) [13,17]. The material retains a low viscosity even at the high monomer conversion degree thus allowing the mass-transport of the components, due to an extra free volume formation in the bright areas. It results in a modulation of a chemical composition. Besides, according to the composition of NOA adhesive [13] and refractive index data from Aldrich database, the main components of NOA mixture have the refractive index difference of  $\approx 0.07$ . The periodic redistribution of the substances with the different refractive indices can provide an increase in the refractive index modulation, especially for smaller periods, less than  $2\ \mu\text{m}$ . The contribution of this process is strongly reduced at large periods. This was actually observed experimentally: both total DE (Fig. 4) and  $n_1$  (Fig. 6) were small for large periods.

In order to further clarify the mechanism of the relief formation an additional experiment allowing to elucidate the position of the valley and grooves in the surface relief at least for larger periods has been performed. The NOA68 film was exposed through the binary mask with different width of the dark and transparent zones (5 and

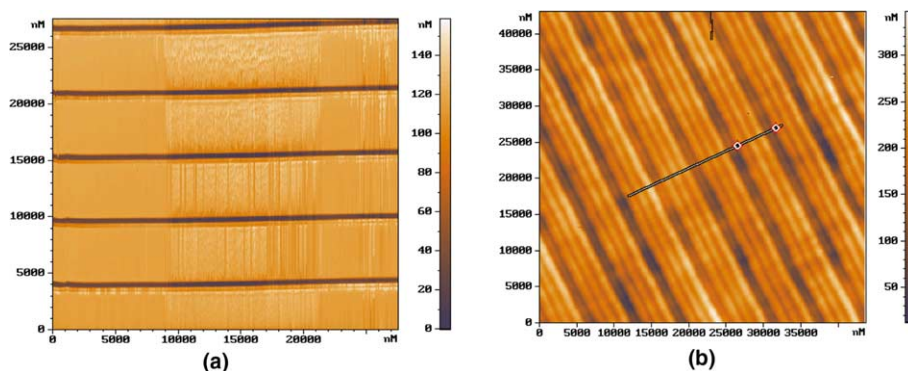


Fig. 9. AFM images (contact-mode) of the surface of: (a) the amplitude mask with different width of the transparent and dark regions, 1 and  $5\ \mu\text{m}$ , respectively; (b) the structure of the NOA68 grating, obtained by the photolithography method through this mask.

1  $\mu\text{m}$ , respectively). The distribution of the light pattern was compared with the obtained relief structure, measured by AFM. Both top views of the mask and the fabricated structure are shown in the Fig. 9. It is obvious that the dark regions of the mask (higher level in AFM image) correspond to the hills on the surface relief. This fact confirms the predominant contribution of the first process (difference of the local density and, consequently, local shrinkage) of relief formation at large periods. The observed experimental fact is in contrast to observed earlier for acrylate-diluents mixture exposed between two glasses [8]. For these mixture the mass-transport of the neutral diluents from the bright to dark regions has a predominant contribution.

As the shrinkage in NOA materials is considerably smaller than in the acrylate mixtures [13,16] this explain well relatively shallow surface relief even for large periods observed in the current investigation.

An extra point in the mechanism is a role of oxygen, dissolved in the reactive mixture [13,16]. Higher efficiency of pure refractive index grating, recorded with free surface compared with the film between two glasses, may be due to the acceleration by oxygen of the thiol-ene addition [13,16].

## 5. Conclusions

In conclusion, we have successfully inscribed and studied permanent holographic gratings into Norland UV-adhesives NOA68. Holographic exposure to Ar-ion laser at 364nm leads to the combination of the volume and surface relief gratings for almost all periods of the structures fabricated. The main role in the formation of the diffraction gratings plays the refractive index modulation and the surface relief modulation almost does not contribute to the total efficiency for the periods less than 2  $\mu\text{m}$ . The depth of the surface relief grows with increase in the grating period and the surface relief modulation gives the dominant contribution into the efficiency of the gratings for the periods larger than 5  $\mu\text{m}$ . The refractive index pattern in NOA68 appears due to the gradients both of the cross-linking density and the

content of the material in the bright and dark regions provided by the photopolymerisation and diffusion of the components during holographic exposure. The difference in the local material shrinkage in the adjacent regions of the grating is suggested as the plausible mechanism of the relief formation. The laser exposure through the mask leads to deep ( $\approx 1\text{--}1.5\mu\text{m}$ ) structures with almost square profile without any subsequent development. NOA68 is the material for the easy single-step holographic or lithographic fabrication of diffractive optical elements without either physical or chemical post-processing.

## References

- [1] T.J. Trout, J.J. Schmiege, W.J. Gambogi, A.M. Weber, *Adv. Mat.* 10 (1998) 1219.
- [2] A.M. Weber, W.K. Smother, T.J. Trout, D.J. Mickish, *Proc. SPIE* 1212 (1990) 30.
- [3] J.R. Lawrence, F.T. O'Neil, J.T. Sheridan, *Optik* 112 (2001) 449.
- [4] S.H. Lin, K.Y. Hsu, W.-Z. Chen, W.T. Whang, *Opt. Lett.* 25 (2000) 452.
- [5] K. Yokoyama, T. Matsuo, H. Tanigawa, *Proc. SPIE* 4659 (2002) 334.
- [6] C. Carre, P. Saint-Georges, C. Lenaerts, Y. Rennotte, *Synth. Mat.* 127 (2002) 291.
- [7] E.S. Gulnazarov, T.N. Smirnova, E.A. Tikhonov, *Opt. Spectr. (Russian)* 67 (1989) 175.
- [8] O.V. Sakhno, T.N. Smirnova, *Optik* 113 (2002) 1.
- [9] G.M. Karpov, V.V. Obukhovskiy, T.N. Smirnova, V.V. Lemesheko, *Opt. Comm.* 174 (2000) 391.
- [10] A. Natansohn, P. Rochon, *Chem. Rev.* 102 (2002) 4139.
- [11] O.A. Kulikovska, K. Charagozloo-Hubmann, J. Stumpe, *Proc. SPIE* 4802 (2002) 85.
- [12] B. Pinto-Iguanero, A. Olivares-Perez, I. Fuentes-Tapia, *Opt. Mat.* 20 (2002) 225.
- [13] L.V. Natarajan, C.K. Shepherd, D.M. Brandelik, R.L. Sutherland, S. Chandra, V.P. Tondiglia, D. Tomlin, T.J. Bunning, *Chem. Mater.* 15 (2003) 2477.
- [14] R.J. Colier, C.B. Burckhardt, L.Y. Lin, *Optical Holography*, Academic Press, NY, London, 1973, 686p.
- [15] D.-J. Lougnot, *Proc. SPIE* 1399 (1993) 10.
- [16] R. Houbertz, G. Domann, J. Schulz, B. Osowski, L. Freuhlich, W.-S. Kim, *App. Phys. Lett.* 84 (2004) 1105.
- [17] A.F. Jacobine, in: J.D. Fouassier, J.F. Rabek (Eds.), *Radiation Curing of Polymer Science and Technology III*, Elsevier Applied Science, London, 1993, p. 219, Chapter 7.